Journal of *Marine Science and Engineering*

MDPI

Article

Numerical Study on the Effect of Port Orientation on Multiple Inclined Dense Jets

Seyed Ahmad Reza Saeidi Hosseini [1], Abdolmajid Mohammadian [1,*], Philip J. W. Roberts [2] and Ozeair Abessi [3]

[1] Department of Civil Engineering, University of Ottawa, 75 Laurier Ave E, Ottawa, ON K1N 6N5, Canada; ssaei041@uottawa.ca
[2] School of Civil and Environmental Engineering, Georgia Institute of Technology, Atlanta, GA 30332, USA; phil.roberts@ce.gatech.edu
[3] School of Civil Engineering, Babol Noshirvani University of Technology, Babol 4714871167, Iran; oabessi@nit.ac.ir
* Correspondence: majid.mohammadian@uottawa.ca

Abstract: Wastewaters are commonly discharged into the seas and oceans through multiport diffusers. Accurate prediction of the complex interactions of multiport diffusers with the receiving water bodies is significant for the optimal design of outfall systems and has yet to be fully illuminated. In the current study, the mixing and dilution characteristics of multiple inclined dense jets are studied using a three-dimensional numerical simulation. The Launder, Reece, and Rodi (LRR) turbulence model is employed to perform the simulations, and the predictions are compared against available experimental data. The results indicate that the LRR turbulence model is a promising tool for the study of inclined dense jets discharged from multiport diffusers, and it can provide more accurate predictions of the mixing behavior than standard and re-normalization group (RNG) k-ε turbulence models. The model is further employed to evaluate and compare the dispersion capabilities of multiport diffusers with uniform and non-uniform jet orientation to the horizontal, as a novel idea. The comparisons demonstrate the middle discharge may have a longer trajectory (7% and 5% increase in terminal rise height and impact point distance, respectively) and therefore a higher dilution rate (14% increase in impact dilution) when its adjacent jets are disposed with a different angle, compared to that of uniform discharges. The outcomes may be favorable for outfall systems applications involving dilution.

Keywords: numerical simulations; multiple discharges; inclined dense jets; mixing and dilution; discharge inclination

check for updates

Citation: Saeidi Hosseini, S.A.R.; Mohammadian, A.; Roberts, P.J.W.; Abessi, O. Numerical Study on the Effect of Port Orientation on Multiple Inclined Dense Jets. *J. Mar. Sci. Eng.* **2022**, *10*, 590. https://doi.org/10.3390/jmse10050590

Academic Editors: Fuping Gao and Alessandro Antonini

Received: 22 March 2022
Accepted: 23 April 2022
Published: 26 April 2022

Publisher's Note: MDPI stays neutral with regard to jurisdictional claims in published maps and institutional affiliations.

Copyright: © 2022 by the authors. Licensee MDPI, Basel, Switzerland. This article is an open access article distributed under the terms and conditions of the Creative Commons Attribution (CC BY) license (https://creativecommons.org/licenses/by/4.0/).

1. Introduction

Brine wastewaters from desalination plants are commonly discharged into the seas and oceans through diffusers. These effluents, which have a density higher than the surrounding water, sink to the sea-bottom and can increase salinity near the diffuser, which can result in adverse effects on the local natural environment if not properly discharged [1]. The mixing characteristics of the wastewater discharges are closely related to the properties of the outfall diffusers [2,3]. Thus, it is essential to predict the mixing behavior of the jets from different kinds of diffusers to enable an economically efficient design while complying with regulatory demands.

Discharges may be positively, neutral, or negatively buoyant. Positively buoyant jets have a density lower than the ambient water density and rise due to a positive buoyancy until they reach the water surface and then spread horizontally as a plume; the horizontal and vertical multiple discharges are typically positively buoyant or neutral. Negatively buoyant jets have a density higher than the surrounding water, and they are affected by a negative buoyancy which hinders the flow moving upward and leads the jets to move

back to the sea bottom; the inclined jets are mainly negatively buoyant. Thus, the trajectory and therefore mixing behavior of inclined jets may differ from the horizontal and vertical discharges, which highlights the importance of the separate study of inclined jets. On the other hand, the diffusers may be either single- or multi-port. Single-port discharges can freely mix with the receiving water without any interactions. However, multiport diffusers are frequently applied around the world, e.g., Melbourne, Perth, Sydney, and Boston, to enable high dilutions with high effluent flow rates [4,5]. The mixing process of multiport discharges differs from single-port jets, and its study is much more complicated because of the complex mechanisms resulting from jet interactions and the Coanda effect. Although the mixing behavior of single inclined dense jets has been widely studied for many years, the dilution properties of multiple jets have received less attention.

The investigations on multiple buoyant jets were quite often experimental or analytical. Some prior experimental studies on multiple buoyant jets have focused on multiple horizontal [5–11] and some others on vertical [4,12] discharges. Some studies analytically investigated multiple buoyant jets and estimated the distance over which the interacting 3D buoyant jets behave as a plane jet [7,13]. Knystautas theoretically predicted the velocity field of multiple turbulent jets using the superposition technique based on the Reichardt hypothesis [6]. Knystautas' model was further improved to predict the concentration field based on an extension of the Reichardt hypothesis to the lateral transport of pollutants [14]. Wang and Davidson [5] argued that the models presented by Knystautas [6] and Hodgson et al. [14] did not capture the possible change in spreading rate due to jet merging, and extended their models by considering the changes in the spreading rates and concentration to velocity length scale ratio between the axisymmetric and 2D flow limits. Yannopoulos and Noutsopoulos analyzed interacting vertical buoyant jets in stagnant ambient conditions, and developed analytical expressions concerning the concentration and velocity distributions based on the entrainment restriction approach [12] and superposition method [15]. Lai and Lee [16] proposed a general semi-analytical model for the dynamic interaction of multiple buoyant jets, and showed that merging point, jet trajectories, as well as the centerline concentration and velocity of the buoyant jet group were perfectly matched with the measurements. Furthermore, multiple inclined discharges have been mainly studied experimentally [17–23].

Although experimental studies have significantly contributed to a better understanding of multiple jets, they are expensive and time-consuming options. Thus, supplementary methods such as integral entrainment models have always been of interest. These models are widely employed by designers to assess jet mixing behavior and are a basis for commercial mixing tools such as JetLag [24,25], CoreJet [26], and UM3 [27]. According to integral entrainment models, the velocity profiles of a jet is assumed to be Gaussian or top hat and axisymmetric without radial changes, resulting in simplified governing momentum and mass conservation equations [28]. These models are unable to resolve re-entrainment, boundary effects, and the Coanda effect [28,29]. The last limitation may shed doubt on the prediction capabilities of integral entrainment models for multiple jets, where the Coanda effect reduces jet dilution and terminal rise height [19,30]. Palomar et al. [31] evaluated the prediction capabilities of the JetLag, CoreJet, and UM3 tools for inclined dense jets. They found a lot of discrepancies for the prediction of terminal rise height, and showed more than 50% under-prediction for dilution. This underestimation has roots in the simplified mass and momentum equations of the integral models resulting from the simplex assumptions for the jet velocity profiles.

Thanks to the advancements in computational resources over the past two decades, the application of computational fluid dynamics (CFD) modeling in the prediction of jet-mixing behavior has dramatically increased [32]. CFD includes fewer simplifying assumptions, compared to integral entrainment models, and is currently a promising approach to simulate desalination outfalls [29]. The application of CFD modeling, including the Reynolds Averaged Navier Stokes (RANS) model [33–38] and large eddy simulation (LES) [39–41], has been reported for single port discharges in recent works. However, there

have been only a limited number of reports covering the predictive capabilities of CFD models for multiple jets. Some studies have numerically investigated multiple buoyant jets. Xue et al. [42] indicated that the standard k-ε model could reasonably predict the mixing behavior of multiple horizontal jets in cross-flow. Tang et al. [43] applied a buoyancy-corrected eddy viscosity model (EVM) to predict the primary mixing of buoyant jets from multiple ports, and compared the results to the CORMIX model predictions. They showed that the CFD model could capture the changes of the plumes' depth along the trajectory, which the CORMIX model was incapable of capturing. Yan et al. [44] investigated the prediction capabilities of four different turbulence closures including the standard k-ε, re-normalization group (RNG) k-ε, k-ω, and k-ω shear stress transport (SST) for multiple vertical jets and showed that (RNG) k-ε resulted in more accurate outcomes. As the mixing behavior of multiple inclined discharges may differ from buoyant jets due to the negative buoyancy, some studies have attempted to validate the application of CFD for those jets. Yan and Mohammadian [3] validated the performance of the standard and re-normalization group (RNG) k-ε turbulence models for the prediction of multiple inclined dense jets and showed that both models could provide predictions of the terminal rise height and the impact point dilution with errors lower than 15%. Moreover, the predictions for the impact distance based on the standard and (RNG) k-ε closures were found to be accurate with errors of 18.6% and 13.3%, respectively. A recent study [29] conducted numerical CFD simulations based on k-ω (SST) closure to investigate the Gold Coast Desalination Plant offshore inclined multiport brine diffuser while affected by different ambient velocity conditions, in the range of 0.03–0.26 m/s, and validated impact dilutions and plume trajectory against physical experimental data.

Experimental and numerical models are adopted to predict the mixing behavior of discharges, which are significantly affected by the properties of outfall diffusers [2,3]. For single dense discharges, inclined jets result in a higher dilution rate than vertical discharges since vertical jets tend to fall back on themselves and it significantly impairs the dilution process [45–47]. It is widely accepted that the 60° inclined discharges provide the longest trajectory for entrainment and therefore the highest dilution rate [48–51]. The effects of flow orientation on the flow field have been also investigated in other hydraulic conditions [52–54]. The main issue with multiple inclined dense discharges arises when the ports are not sufficiently spaced apart, and the jets are closely or moderately spaced. The dynamic interaction and the Coanda effect cause these jets to have a reduced terminal rise height and to bend inward, and thus to have a shorter trajectory compared to a single jet [19]. The shortened trajectory further decreases dilution since it diminishes the available surface for entrainment. To overcome this reduction in dilution, it has been recommended to space the jets sufficiently apart in multiport diffusers [19], which lets the jets freely entrain the surrounding water without any interactions, as single jets do. The effect of port spacing on the mixing process of multiport diffusers has been the focus of some prior research. Yan et al. [44] focused on multiple vertical buoyant jets and indicated that as the port spacing was reduced, the jets' centerline dilution was lower, and the plume-like region was placed farther from the port. Moreover, they proposed a novel formula for concentration profiles that considers the influence of port spacing. Abessi and Roberts [19] conducted laboratory experiments on the influences of port spacing on multiple inclined dense jets and indicated that the port spacing can have a negative effect on the rise height and other geometrical characteristics of discharges. They highlighted the minimum port spacing that avoids dynamic interaction of jets.

Based on the above explanations, two main research gaps need to be further elaborated when focusing on the study of multiport diffusers. First evaluating the prediction capabilities of less validated modeling approaches, from the CFD simulation point of view, and secondly investigating the influence of non-uniform port orientation on the mixing behavior, from the optimal design point of view. The available numerical studies have mainly investigated the prediction capabilities of the eddy viscosity models (EVMs). The EVMs consider that the Reynolds stresses are proportional to mean rates of deformation and the

stresses are obtained based on the Boussinesq assumption [55]. These models provide good results for simple flows and some recirculating flows [55], but some drawbacks have been reported for them when employed for complex flow fields [56,57]. The main drawback of most EVMs can be the consideration of isotropic character for the eddy viscosity, which causes them to be insensitive to the orientation of the turbulence structure and its mixing and transport processes [35]. However, the stress anisotropy plays a significant role in changing in the streamline trajectory and stress-induced secondary motions [57]. The RSMs solve transport equations for the Reynolds stresses and consider different values for viscosity in each direction, which may result in more accurate predictions compared to the EVMs for the complex flow fields [55]. Gildeh et al. [35] applied five different RANS models, including the re-normalization group (RNG) k-ε, realizable k-ε, nonlinear k-ε, Launder, Reece, and Rodi (LRR), and Launder-Gibson, to predict the mixing behavior of 30° and 45° inclined dense jets. They showed that the two RSMs could provide more accurate predictions for the velocity fields compared to the other applied models. Additionally, the LRR model could better capture secondary flows. It is likely that the RSMs will begin to be more widely applied for industrial projects once a consensus has been achieved about the best numerical solution strategies for their convergence problems [55]. Additionally, the advances in computational resources in the early future may lead these models to be more employed by industrial users. Therefore, this study simulates multiple inclined dense discharges employing the Launder, Reece, and Rodi (LRR) model as a new approach for multiple jets, and compares the model predictions of terminal rise height, impact point distance, and impact dilution to existing experimental measurements.

Furthermore, previous studies have mainly focused on the influence of port spacing on the mixing characteristics of multiport diffusers. However, the influence of non-uniform port orientation on the merging process of multiport diffusers is rarely reported. Jet merging in multiport diffusers leads the jets to have shorter trajectories and lower dilution compared to single jets. It is expected that the jet merging and the Coanda effect diminish when the jets are discharged with non-uniform orientation to the horizontal, compared to uniform discharged diffusers. A change in port orientation can be of interest in practical projects, such as brackish water discharges into water bodies emitted by osmotic power plants, since it may provide an inexpensive way to enhance the mixing performance. Thus, as another contribution of this study, the effect of non-uniform port orientation on the merging process of multiple inclined dense jets is also evaluated using the validated LRR model.

The rest of this paper is devoted to the description of research methodology as well as presenting and discussing the results and conclusions. Section 2 describes methodology where dimensional analysis, governing equations, flow and mesh configurations, as well as model setup and numerical algorithms are discussed. Section 3 presents the results where the performance of the model and the effect of non-uniform port orientation on merging process are discussed. Section 4 also presents the conclusion and proposed future works.

2. Methodology

2.1. Analysis

A schematic view of multiple inclined dense jets is illustrated in Figure 1. The jets are discharged into the receiving water bodies at an initial angle θ to the horizontal with jet velocity U_0 and jet diameter D. Upon discharging, the jets move upward due to the initial vertical momentum flux. The negative buoyancy and jet entrainment continuously decrease this momentum flux until it almost vanishes at the point where the jets reach their maximum height, the terminal rise height y_t. Subsequently, the jets turn downward and impinge the seabed at the location of impact point, x_i. The dilution at the impact point S_i can be defined as $S_i = (\rho_0 - \rho_a)/(\rho - \rho_a)$, where ρ_0 is effluent density, ρ_a is ambient density, and ρ represents local density.

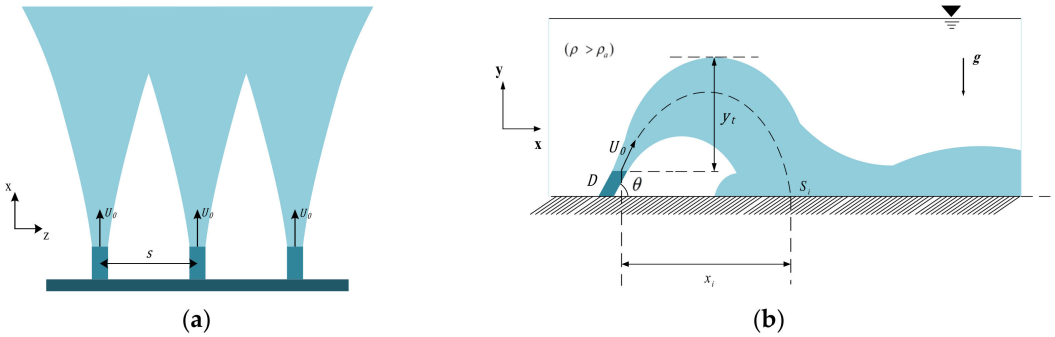

Figure 1. Schematic (**a**) plan and (**b**) side views of multiple inclined dense jets.

The mixing properties of the inclined dense jets are mainly characterized by discharge volume flux Q, kinematic momentum flux M, and buoyancy flux B, which can be defined by the following equations, respectively [28,45,58,59]:

$$Q = \frac{\pi D^2}{4} U_0;\ M = U_0 Q = \frac{\pi D^2}{4} U_0^2;\ B = g_0' Q \tag{1}$$

where g_0' is reduced gravitational acceleration and expressed as $g_0' = g(\rho_0 - \rho_a)/\rho_a$; where g is gravitational acceleration. In the case of dense discharges $\rho_0 > \rho_a$.

The most important length-scale of the flow is the momentum length scale, L_M, which refers to the distance beyond which the buoyancy produces momentum approximately equal to the initial momentum and is defined as [46,60]

$$L_M = \frac{M^{3/4}}{B^{1/2}} \tag{2}$$

which is commonly expressed as DF_d where F_d is the jet densimetric Froude number, which measures the ratio of inertia to buoyancy and can be defined as

$$F_d = \frac{U_0}{\sqrt{g_0' D}} \tag{3}$$

The effect of port spacing in dimensional analysis is expressed by the non-dimensional parameter s/DF_d where s is the port spacing. If the ports are widely spaced, $s/DF_d > \sim 2$, the jets behave as single jets and freely mix with the ambient water. If a single jet is fully turbulent and F_d is higher than approximately 20, the dynamic effect of Q becomes insignificant. Therefore, the dependent variables of y_t, x_i, and S_i are functions of M and B only. Following a dimensional analysis and experimental measurements [46]

$$\frac{y_t}{DF_d} = 2.2;\ \frac{x_i}{DF_d} = 2.4;\ \frac{S_i}{F_d} = 1.6 \tag{4}$$

For the case that the jets are not widely spaced, $s/DF_d < \sim 2$, the right-hand sides of Equation (4) are not constant anymore. The geometrical characteristics and impact dilution are functions of s/DF_d, as follows

$$\frac{y_t}{DF_d} = f\left(\frac{s}{DF_d}\right);\ \frac{x_i}{DF_d} = f\left(\frac{s}{DF_d}\right);\ \frac{S_i}{F_d} = f\left(\frac{s}{DF_d}\right) \tag{5}$$

Following the experiments conducted by Abessi and Roberts [19], the normalized terminal rise height and impact distance for one- and two-sided multiport discharges can be obtained by the empirical equations

$$\frac{y_t}{DF_d} = 1.9\left(\frac{s}{DF_d}\right)^{\frac{1}{2}};\ \frac{x_i}{DF_d} = 2.0\left(\frac{s}{DF_d}\right)^{\frac{1}{2}} \tag{6}$$

The impact dilution for one-sided multiport diffusers can be achieved by

$$\frac{S_i}{F_d} = 0.9\left(\frac{s}{DF_d}\right) \tag{7}$$

while for two-sided discharges it is about 20% lower.

2.2. Governing Equations

The mass and momentum conservation equations for an incompressible multiphase flow are as follows [61,62]:

$$\nabla \cdot U = 0 \tag{8}$$

$$\frac{\partial \rho U}{\partial t} + \nabla \cdot (\rho UU) = -\nabla \cdot \left(P_{rgh}\right) - gh\nabla\rho + \nabla \cdot (\rho T) \tag{9}$$

where

$$\rho = \alpha_1\rho_1 + \alpha_2\rho_2 = \alpha_1\rho_1 + (1-\alpha_1)\rho_2 \tag{10}$$

$$\mathrm{T} = -\frac{2}{3}\overline{\mu}_{eff}\nabla \cdot \mathrm{UI} + \overline{\mu}_{eff}\nabla\mathrm{U} + \overline{\mu}_{eff}(\nabla\mathrm{U})^{\mathrm{T}} \tag{11}$$

$$\overline{\mu}_{eff} = \alpha_1\left(\mu_{eff}\right)_1 + \alpha_2\left(\mu_{eff}\right)_2 \tag{12}$$

$$\left(\mu_{eff}\right)_i = (\mu - \mu_t)_i \tag{13}$$

where U is velocity, t indicates time, ρ is density, P_{rgh} represents the difference between static and hydraulic pressure, g is gravitational acceleration, h denotes height of fluid column, α is volume fraction, μ and μ_t are dynamic and turbulent viscosity, respectively, script i shows either the effluent ($i = 1$) or surrounding water ($i = 2$). The diffusion equation for the volume fraction of a fluid can be written as:

$$\frac{\partial \alpha_1}{\partial t} + \nabla \cdot (U\alpha_1) = \nabla \cdot \left(\left(D_{ab} + \frac{\nu_t}{S_C}\right)\nabla\alpha_1\right) \tag{14}$$

where D_{ab} indicates molecular diffusivity, ν_t represents turbulent eddy viscosity, and S_C denotes turbulent Schmidt number.

In CFD modeling, the three approaches of direct numerical simulation (DNS), LES, and RANS models can be used to simulate turbulent flows. The first two requires excessive computational cost for the simulation of multiple jets. The RANS models can be classified into the RSMs and EVMs. The RSMs usually need more computational resources. One study applied three different EVMs and two RSMs to predict the mixing behavior of single jets and showed that the RSMs were about 20% more expensive than the other models, regarding the computational costs [35]. However, the RSMs may be more accurate when the flow field is complex, which has roots in dealing with stress anisotropy [55]. The main difference between the RSMs and EVMs is that RSMs directly solve transport equations for the Reynolds stress, as presented in Equation (15), while the EVMs compute the stresses using the Boussinesq assumption. This difference may lead to more accurate predictions of the mixing behavior of multiple jets using an RSM compared to an EVM. In the current

study, the LRR model, as an RSM, is adopted to solve the governing equations. The LRR model was developed by Launder, Reece, and Rodi in 1975 [63] and is expressed as:

$$\frac{D\overline{u_i u_j}}{\mathrm{Dt}} = \frac{\partial \overline{u_i' u_j'}}{\partial t} + \overline{u_k}\frac{\partial \overline{u_i' u_j'}}{\partial x_k} = D_{ij}^T + D_{ij}^\nu + P_{ij} + \phi_{ij} + \varepsilon_{ij} \tag{15}$$

where $\overline{u_i' u_j'}$ is the Reynolds stress, and D_{ij}^T, D_{ij}^ν, P_{ij}, ϕ_{ij}, and ε_{ij} represent the turbulent diffusion, viscous diffusion, production, pressure–strain, and turbulence dissipation rate parameters, respectively. The viscous and turbulent diffusion terms are calculated as

$$D_{ij}^\nu = \nu\frac{\partial^2 \overline{u_i' u_j'}}{\partial x_k x_k} \tag{16}$$

$$D_{ij}^T = \frac{\partial}{\partial x_l}\left(C_s\frac{\varepsilon}{k}\overline{u_i u_k}\frac{\partial \overline{u_i u_j}}{\partial x_k}\right) \tag{17}$$

where $C_s = 0.22$, and the pressure–strain term is expressed as

$$P_{ij} = -\overline{u_i' u_k'}\frac{\partial \overline{u_j}}{\partial x_k} - \overline{u_j' u_k'}\frac{\partial \overline{u_i}}{\partial x_k} \tag{18}$$

The dissipation term is calculated as

$$\varepsilon_{ij} = -2\nu\overline{\frac{\partial u_i'}{\partial x_k}\frac{\partial u_j'}{\partial x_k}} \tag{19}$$

$$\frac{\partial \varepsilon}{\partial t} + \overline{u_k}\frac{\partial \varepsilon}{\partial x_k} = C_{\varepsilon 1}\frac{P_k \varepsilon}{k} - C_{\varepsilon 2}\frac{\varepsilon^2}{k} + \frac{\partial}{\partial x_j}\left(C_\varepsilon\frac{k}{\varepsilon}\overline{u_i' u_j'}\frac{\partial \varepsilon}{\partial x_j}\right) \tag{20}$$

where $C_{\varepsilon 1} = 1.44$, $C_{\varepsilon 2} = 1.90$.

2.3. Flow and Mesh Configurations

As the purpose of the current study was to evaluate the predictive capabilities of RSM for multiple inclined dense jets and investigate the effects of non-uniform port orientation to the horizontal on the mixing behavior, previous experiments were first simulated to validate the LRR model predictions. The experiments conducted by Abessi and Roberts [19] were selected as a basis for model validation, and the results of their measurements and LRR simulations were compared. Their measurements were appropriate for model validation since concentration fields were mapped in three dimensions by laser-induced fluorescence, and a comprehensive dataset on multiport inclined dense effluents was provided. Afterward, the validated model was utilized for further investigations on the effects of non-uniform port angle on the mixing process. According to the experiments, the port spacing (s) was 57 mm, the jet diameter (D) was 1.93 mm, and the nozzle height above the lower wall (y_0) was 30 mm. The effluent and tank water density were 1013.8 kg/m^3 and 999.8 kg/m^3, respectively.

To model a long diffuser with many nozzles, three ports were considered in the computational domain as the representatives of all possible jets on a diffuser. Overall, five cases were considered for the simulations, see Table 1. Cases C1, C2, C3, and C4 were utilized for model validation, and were exactly the same as the experimental measurements conducted by Abessi and Roberts [19]. In these cases, s/DF_d varies between 0.47–0.85 to cover moderately spaced ports, which was the focus of this study, and all F_d values were more than 20 to assure fully turbulent flow. In the simulations, the three considered ports were discharged with an angle of 60° to the horizontal, which represents the first configuration (60°–60°–60°). In case S1, the second configuration (45°–60°–45°) is simulated where the central jet is discharges with an angle of 60° to the horizontal and the adjacent jets are discharged with an angle of 45°. Case S1, which has similar conditions to case

C2 except port inclinations, and case C2 were compared to evaluate the effects of port orientation on the mixing process of multiple inclined dense discharges.

Table 1. Characteristics of numerical cases.

Case	Diameters (mm)	Effluent Density (kg/m^3)	Ambient Density (kg/m^3)	Velocity (m/s)	F_d	s/DF_d	θ_1-θ_2-θ_3 (°)
C1	1.93	1013.8	999.8	1.03	63.1	0.47	60-60-60
C2	1.93	1013.8	999.8	0.92	56.8	0.52	60-60-60
C3	1.93	1013.8	999.8	0.85	52	0.57	60-60-60
C4	1.93	1013.8	999.8	0.57	34.7	0.85	60-60-60
S1	1.93	1013.8	999.8	0.92	56.8	0.52	45-60-45

The three considered jets could reflect the mixing behavior of the jets in the whole system using appropriate boundary conditions. The simulations were conducted in a rectangular domain with the dimensions of 600 mm length (along x-direction), 400 mm depth (along y-direction), and 171 mm width (along z-direction); similar domains have been used in many hydraulic simulations [64–66]. The computational domain was surrounded by four types of planes, including wall, outlet, free surface, and symmetry planes. Furthermore, the nozzles were defined by two sections, including nozzle tube and inlet (Figure 2).

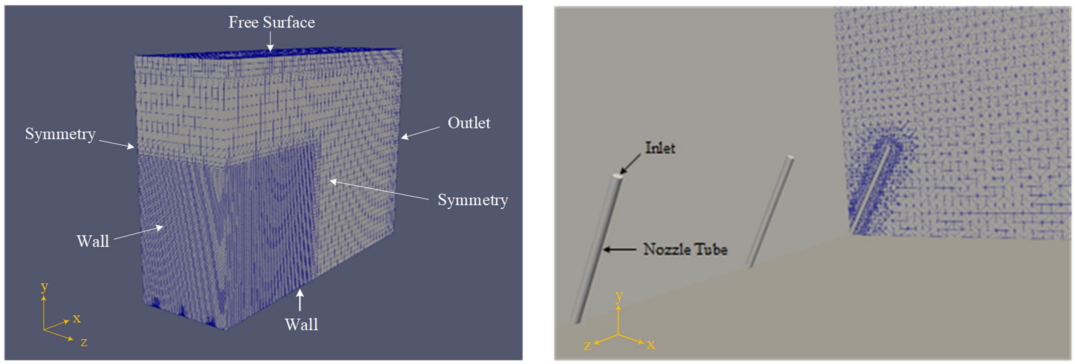

(**a**) (**b**)

Figure 2. (**a**) Computational domain and mesh setup; (**b**) detailed grids near the nozzles.

The accuracy and stability of numerical calculations of fluid flows are significantly affected by boundary conditions. As the wall planes and nozzle tubes are solid surfaces, a no-slip boundary condition was imposed on them to assume zero velocity at those surfaces. The boundary condition at the free surface and outlet planes was set to pressure–inlet outlet velocity. This boundary condition assigns a zero gradient condition for flow into the domain and a velocity, based on the flux in the path-normal direction, for flow out of the domain [67]. A fixed value of velocity was assigned to the inlets, and the initial k and ε values at the inlets were estimated based on [37], $k = 0.06u^2$ and $\varepsilon = 0.06u^3/D$. To simulate the system, the domain was discretized using the structured mesh shown in Figure 2. The mesh was modified by snappyHexMesh tool in OpenFOAM, which can divide the original grids into multiple sub-grids and snap the sub-grid boundaries onto the surfaces of interest. The employment of snappyHexMesh significantly decreased the required number of cells and therefore simulation time since there was no need to have small cells at the regions far from the area of interest. A double refinement was performed for the area in which jets move and merge, and a triple refinement was considered for the grids close to the inlets and nozzle tubes, which could perfectly determine the circular shape of the nozzles. The sensitivity of the simulation outcomes to the cell size was evaluated based on the procedures described and applied by Yan and Mohammadian [68,69]. Simulations were conducted based on four different meshes, including coarse and fine grids. The preliminary mesh structure was a

relatively coarse mesh with 114,000 cells, and the difference between the predictions based on that mesh structure and experimental measurements were found to be about 10%. The finer mesh structures, Mesh 2, Mesh 3, and Mesh 4 included 311,000 cells, 385,000 cells, and 528,000 cells, respectively. The difference between the obtained results using Mesh 2 and Mesh 1 was about 10.5%. However, the difference between the predictions based on Mesh 2 and Mesh 3 was about 1.5%. The predictions of Mesh 3 and Mesh 4 were also very close, with about 2% difference between the results. Therefore, Mesh 4 was selected for simulations, and the final mesh structure included 528,000 cells.

2.4. Model Setup and Numerical Algorithms

The governing equations were numerically solved using the finite volume method. The simulations were performed using an open source code OpenFOAM [70], and the solver twoLiquidMixingFoam was employed to perform the implementation in OpenFOAM. This solver is a transient solver for multiphase fluids and has been widely applied and validated in prior research [2,3,39,41,44,71]. The Gauss linear scheme was adopted for the discretization of the gradient and Laplacian terms, the Euler scheme was utilized to discretize the temporal terms, and the Gauss upwind, Gauss vanleer, and Gauss linear schemes were employed to discretize the divergence terms. The adopted algorithms to solve the coupled pressure and momentum equations were PIMPLE algorithms, see Figure 3. The preconditioned conjugate gradient (PCG) and preconditioned bio conjugate gradient (PBiCG) methods were employed for the pressure field and the other fields, respectively.

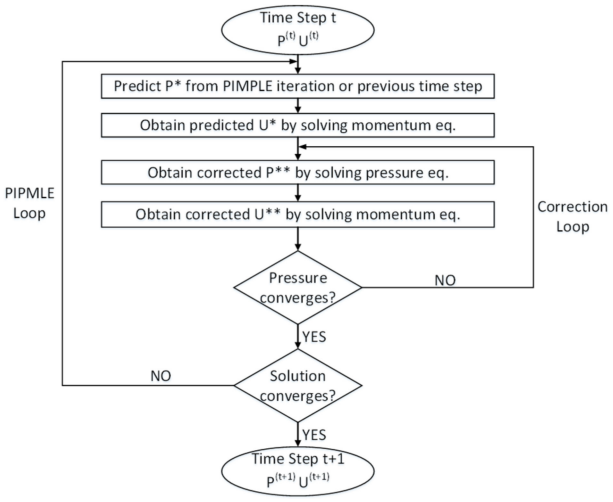

Figure 3. Flowchart of the PIMPLE algorithm; * and ** correspond to predicted and corrected fields, respectively.

The Courant number, C, can be defined as $C = U\Delta t/\Delta x$, where U is flow velocity, Δt represents time step, and Δx indicates cell size. The time step was adjusted during the simulations, and the maximum courant number was set to be 0.5 to provide small time steps. The simulations were run for 120 s, and the results obtained by time-averaging over the period of 70 s to 120 s to ensure fully-developed flow and stable results. Figure 4 shows the time-series graphs for the velocity field along the trajectory of the central jet of case C2. To accelerate the simulation process, the numerical domain was decomposed into 16 regions, 4 parts in x- and 4 part in y-directions, and then each region was processed by a processor. Afterward, the entire domain was reconstructed and the results were extracted. All the computations were performed in the advanced research computing (ARC) systems of Compute Canada, and the real-time computing duration was ranged from 3 to 4 days.

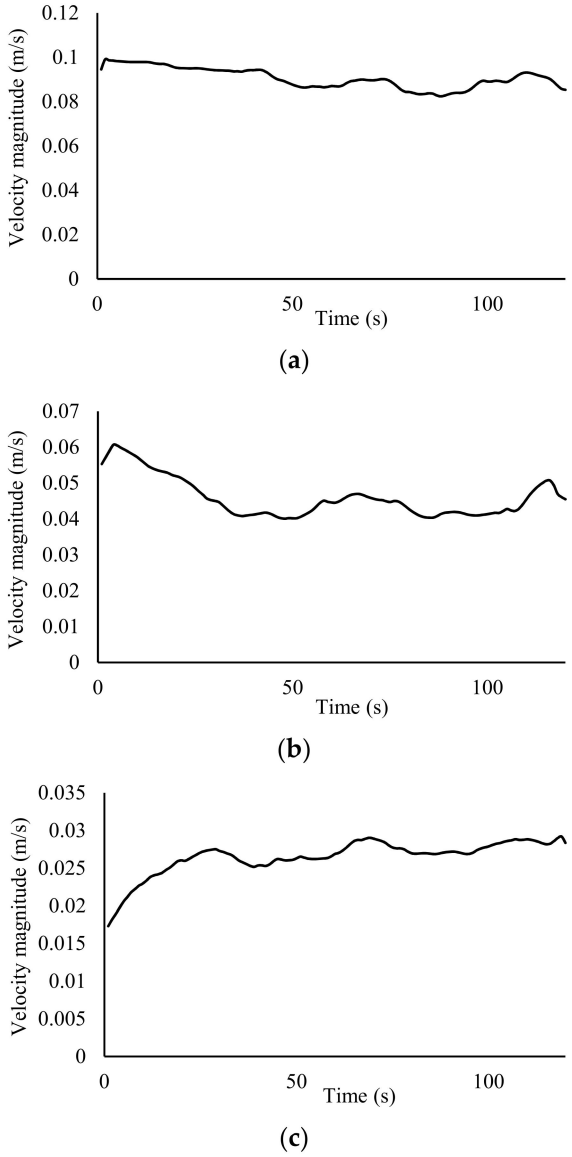

Figure 4. Time-series graphs for the velocity magnitude along the trajectory of the central jet in case C2 at (**a**) $x/(D.F_d) = 0.4$, (**b**) $x/(D.F_d) = 0.75$, and (**c**) $x/(D.F_d) = 1.2$.

To discuss the numerical results in the context of the literature, the accuracy of LRR predictions were compared with that of standard and (RNG) k-ε models adopted for the simulation of the same experimental work in a previous study [3]. Table 2 demonstrates the simulation characteristics of the previous and current study. It is worth mentioning that the numerical results obtained in both studies were mesh-independent, and adopting finer mesh does not necessarily lead to more accurate results. Therefore, the comparison of the accuracy of outcomes can provide a good insight into the performance of the turbulence models.

Table 2. Simulation characteristics of the previous [3] and present study.

	[3]	Current Study
Boundary conditions		
Bottom wall	Slip *	No-slip
Symmetry planes	Symmetric	Symmetric
Inlets	Fixed velocity inlet	Fixed velocity inlet
Atmosphere	Inlet–outlet	Pressure–inlet outlet
Outlet	Inlet–outlet	Pressure–inlet outlet
Number of cells	113,400	528,000
Software	OpenFOAM	OpenFOAM
Solver	twoLiquidMixingFoam	twoLiquidMixingFoam
Discretization schemes		
Temporal term	Euler	Euler
Gradient term	Linear	Linear
Laplacian term	Linear	Linear
Divergence term	Linear, vanLeer, and upwind	Linear, vanLeer, and upwind

* The results were the same when using slip or no-slip boundary condition for the bottom wall [3].

3. Results and Discussion

3.1. Model Validation

The four cases of C1, C2, C3, and C4, moderately-spaced discharges, $0.47 < s/DF_d < 0.85$, with different Froude numbers were numerically simulated by the LRR model, and the model predictions for the terminal rise height, impact distance, and impact dilution were compared to the measurements conducted by [19].

Terminal rise height is determined as where the vertical momentum flux almost vanishes along the jet trajectory [35]. However, the y_t value is not defined exactly the same in previous studies. For instance, Lai and Lee [59] defined it as where the concentration was 25% of the local maximum height concentration, C, while the integral model CorJet applied two cut-off levels, 3% and 25%, for the visual boundary [26]. Shao and Law [72] also adopted the cut-off level of 3%. The definition of y_t in the current simulations was considered to be the locus of 10% of the transverse maximum concentration at the location of jet maximum height, as it was defined in the experimental data [19]. Figure 5 demonstrates the results of normalized terminal rise height, $y_t/(DF_d)$, versus port spacing values, s/DF_d, including cases C1–C4. The value of $y_t/(DF_d)$ for single jets were also included in this figure [46]. The numerical results of terminal rise height were in good agreement with the experimental data. The forecasting accuracy of the model was quantified using mean absolute percentage error (MAPE), the same as in the study conducted by [3], where it was found to be 4.5%. The comparison of $y_t/(DF_d)$ values for cases C1–C4 and single ports showed that the terminal rise height of multiple inclined jets was lower than that of single discharges, which highlights the effect of jet merging. The LRR results for terminal rise height showed slight over prediction compared to the empirical equation, Equation (6), obtained based on the measurements for one- and two-sided multiport diffusers. However, the prediction of terminal rise height at $s/(DF_d) = 0.85$ was matched with Equation (6).

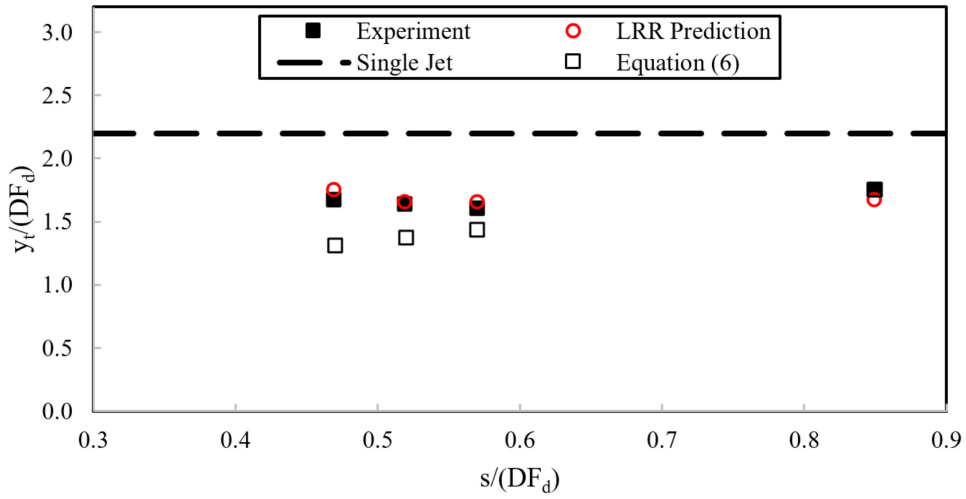

Figure 5. Experimental measurements [19] and numerical results of the normalized terminal rise height.

Figure 6 illustrates the results of normalized impact distance, $x_i/(DF_d)$, versus port spacing values. The model predictions of x_i/D demonstrated a good match with the measurements as the prediction error based on MAPE was less than 4%. The values of $x_i/(DF_d)$ increased with increasing values of port spacing, and all values were lower than the constant value presented for single discharges, $x_i/(DF_d) = 2.4$ [46]. Jet merging causes multiple inclined jets to bend inward, which results in lower impact distance compared to that of single discharges. However, single jets mix with the surrounding water without any intervention. As $s/(DF_d)$ decreases, this effect is more pronounced, and the value of $x_i/(DF_d)$ decreases. The LRR predictions showed higher values for impact distance compared to the general empirical equation for one- and two-sided multiple dense jets.

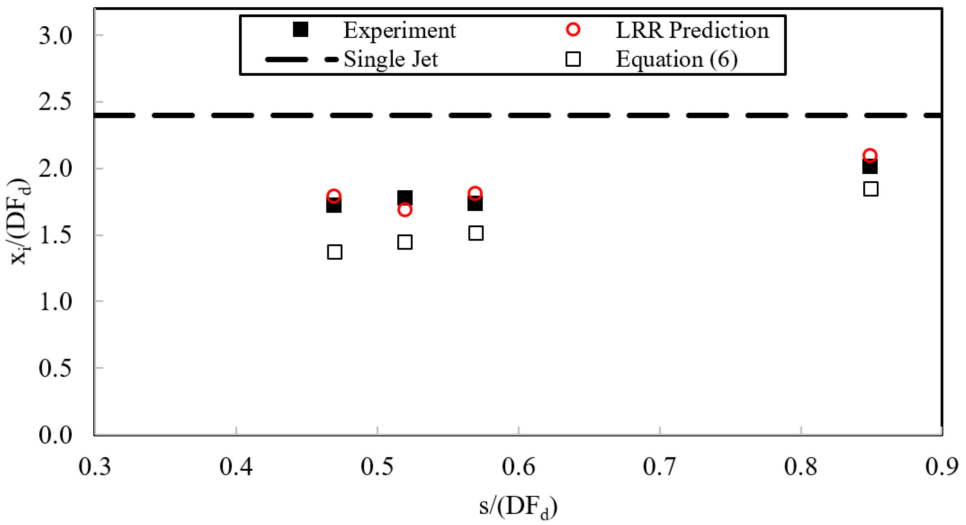

Figure 6. Experimental measurements [19] and numerical results of the normalized impact point distance.

Figure 7 indicates the results of the normalized impact dilution, S_i/F_d, against $s/(DF_d)$. The predictions were in an acceptable range of accuracy, with a MAPE value of 7%. As can be seen, $s/(DF_d)$ had a positive effect on S_i/F_d since the jet merging effect decreased for higher values of $s/(DF_d)$. Furthermore, the values of S_i/F_d were much lower for multiple

discharges compared to single jets. The LRR results were in good agreement with the empirical equation presented for one-sided multiport diffusers, Equation (7).

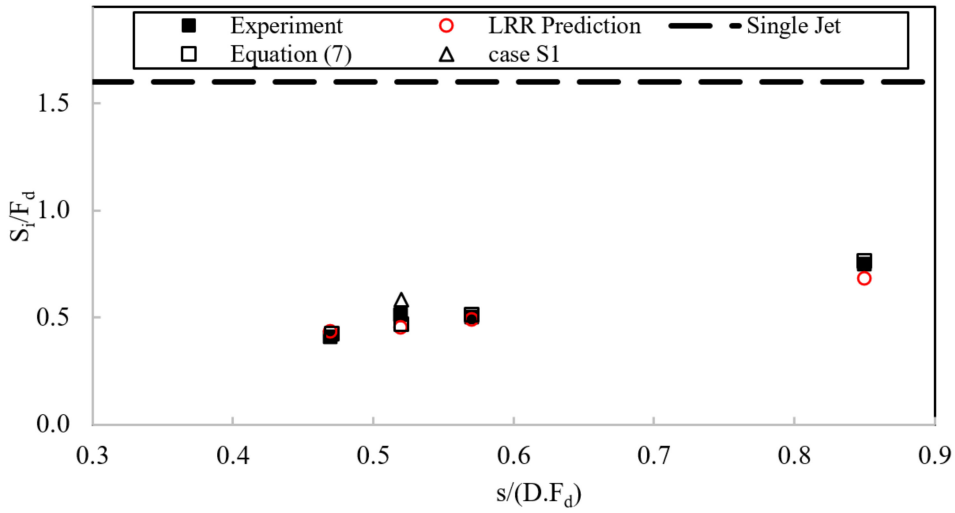

Figure 7. Experimental measurements [19] and numerical results of the normalized impact dilution.

Therefore, the numerical results demonstrated that LRR model, as an RSM, may be a reliable tool for the prediction of mixing behavior of multiple inclined dense jets, as it predicted the geometrical characteristics and impact dilution with mean absolute percentage errors of less than 5% and 7%, respectively. This model provided more accurate predictions compared to the EVMs employed for the simulation of same experimental work [3], see the simulation characteristics in Table 2. It has been shown that RNG k-ε closure may provide results with errors within the range of 15%, and the predictions based on this model were more accurate compared to the standard k-ε closure [3]. The reason behind the higher accuracy of LRR predictions may have its roots in the main difference between RSMs and EVMs: RSMs directly solve the Reynolds stresses, while EVMs model them. In particular, EVMs consider that Reynolds stresses are proportional to mean rates of deformation [55]. It has been also mentioned that RSMs may perform better relative to EVMs when the flow fields are sophisticated [55]. Although the employment of the LRR model for the simulation of multiple jets has rarely been reported, one study focusing on 30° and 45° single inclined dense jets highlighted the outperformance of the LRR model over the RNG k-ε and nonlinear k-ε models [35].

3.2. Effect of Non-Uniform Port Orientation on Jet Merging Process

As a novel contribution to the literature, the effect of non-uniform port orientation on jet merging process was investigated by comparing cases C2 and S1. Case C2 refers to a diffuser with uniform port orientation to the horizontal, including three jets which are discharged with an angle of 60°. In case S1, the central jet is discharged with an angle of 60°, and the adjacent jets with an angle of 45°. The volume fraction, α, in the governing equations is the normalized concentration, C/C0, obtained in post-processing, where C is the local concentration and C0 is the initial concentration. Figure 8 demonstrates the general shape of the jets for cases C2 and S1, and also the vertical slices where the data were extracted. In both cases, the jets moved upward due to the vertical component of the initial momentum, and this momentum continuously decreased due to jet entrainment and negative buoyancy until it equaled zero. Afterwards, the dense jets moved downward and subsequently impacted the bottom boundary. Unlike case C2, the central jet of the diffuser with non-uniform jet orientation to the horizontal, case S1, had higher y_t and lower x_i compared to its adjacent jets, which were discharged with an angle of 45° to the horizontal. This occurred because of the difference between the components of initial momentum of 45° and 60° inclined jets.

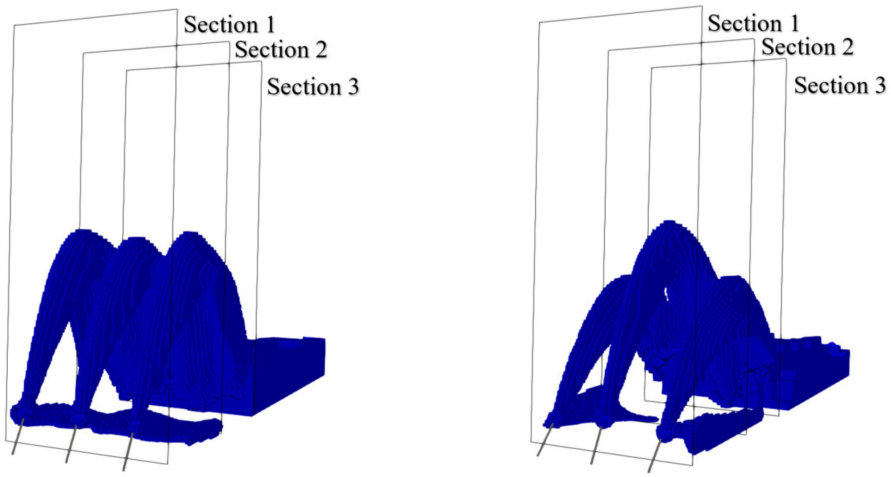

Figure 8. Visualization of (**a**) uniform (case C2) and (**b**) non-uniform (case S1) inclined dense jets, using a velocity isosurface (U = 0.015 m/s).

To investigate the jet merging process for the two different cases, concentration profiles at cross-sections close to and far from the nozzles were extracted, see Figure 9. Close to the ports, e.g., Figure 9a, the jets in both cases seemed to be completely separate, like single jets, with high concentration at the jet centers, and they were not wide enough to interact with each other. Along the trajectory, the jets became more diluted due to the entrainment of the surrounding water, due to shear induced entrainment at the jets' edges. Farther away, e.g., Figure 9b, the maximum concentrations were significantly decreased compared to Figure 9a, and the jets were more diffused. The distance between the jet's centers in case S1 are more than that of case C2 because of the difference between the jets' elevation in case S1. Different orientations of the ports provide more space for the central jet to expand before interacting with other jets. As shown in Figure 9b, at $x/(D.F_d) = 1.5$, the jets in case C2 were almost merged, and there was no space between them or under the central jet. This means the entrainment of fresh water into the jet was restricted in the z-direction and y-direction, from the lower edge. However, there were still some areas with almost zero concentration around the central jet in case S1. It is worth mentioning that the entrainment was restricted in both cases and, therefore, dilution was less than that of single jets. Eventually, in case C2, the individual jets were indistinguishable after the impact point of the central jet, see Figure 9c. However, there was still a trace of 45° inclined dense jets in case S1.

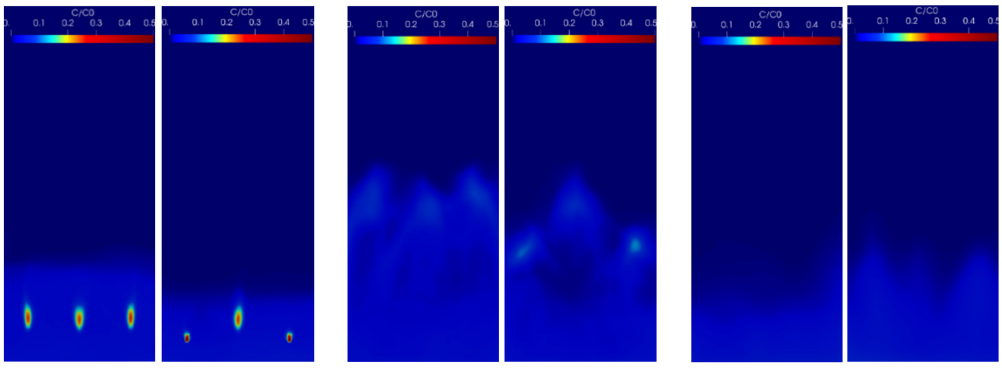

Figure 9. Concentration fields at different cross sections of uniform (case C2) and non-uniform (case S1) multiple inclined dense jets; (**a**) Section 1 ($x/(D.F_d) = 0.25$); (**b**) Section 2 ($x/(D.F_d) = 1.5$); (**c**) Section 2 ($x/(D.F_d) = 2.5$).

Jet merging may be the main source of difference between the mixing characteristics of single and multiple discharges. The Coanda interaction between the rising and descending parts of a dense jet causes the rising jet to attempt to re-entrain itself. As the jets are closely- or moderately-spaced, jet merging results in a virtually impenetrable wall that prevents the entrainment of ambient water to inner surfaces and intensifies the Coanda effect. The lack of clear water on inward faces causes the jets to bend inward more sharply in search of clear water [19]. Thus, multiple dense jets usually have shorter trajectories and therefore lower dilution rates compared to single jets. This difference between single and multiple jets can be also observed between the diffusers with uniform and non-uniform port orientation. Figure 10 indicates the contours of normalized concentration fields at the central planes for cases C2 and S1. The contours in both cases showed that the lower part of the jet was more expanded compared to the upper part. As shown in Figure 10, the central jet in case C2 bent inward more sharply, and there was less available clear water (C < 0.02 C0) under the central jet when the discharges were uniform, compared to that of non-uniform jets. It was found that the impact dilution for case S1 was 14% higher than that of case C2, see Figure 7. The availability of more clear water at the inner edge of the jet in case S1, compared to that of C2, decreased the entrainment restriction and thus caused higher dilution rates.

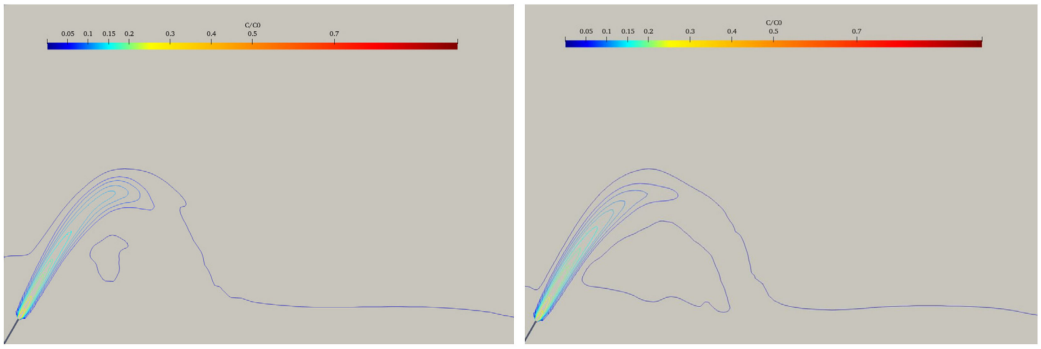

(**a**) (**b**)

Figure 10. Concentration contours at the central plane for (**a**) case C2 and (**b**) case S1.

A comparison of central jet trajectories more clearly highlights the effect of adjacent jets on the geometrical characteristics of central jets. As shown in Figure 11a, the trajectory of the central jet in case S1 was at a lower elevation, compared to case C2, before the terminal rise height. However, it reached higher elevations after the terminal rise height and did not bend inward as sharply as the other case, demonstrating the reduced effect of jet merging and the Coanda interaction. The terminal rise height and impact point distance were found to be 7% and 5% higher for case S1 relative to case C2. A small deviation between the trajectories before the terminal rise height may be attributed to the Coanda interaction between the jets. The jets mutually attempted to entrain one another because of a pressure force, resulting from a change in the entrained flow pattern, that moves a jet to the other jet [19]. This effect can be seen in a study focusing on multiple positive buoyant jets [73] where the end plumes bend inwards as a result of unbalanced inward pressure force on the plumes, while the central jets move vertically because of the equally balanced forces on each side of them. Similarly, in case S1, as the adjacent jets are at a different elevation, the induced low-pressure field differs from that of case C2. As the central jet tries to entrain into the adjacent ones, which are at a lower elevation, it becomes somewhat deflected. Figure 11b illustrates how the concentration changes along the trajectory of the central jet in case S1 and case C2. As shown, before the terminal rise height, the concentration of the central jet in case C2 was lower than that for case S1. However, beyond this point, where the jets in case C2 interacted with each other and there was limited fresh water around the jets, its concentration became lower compared to case S1.

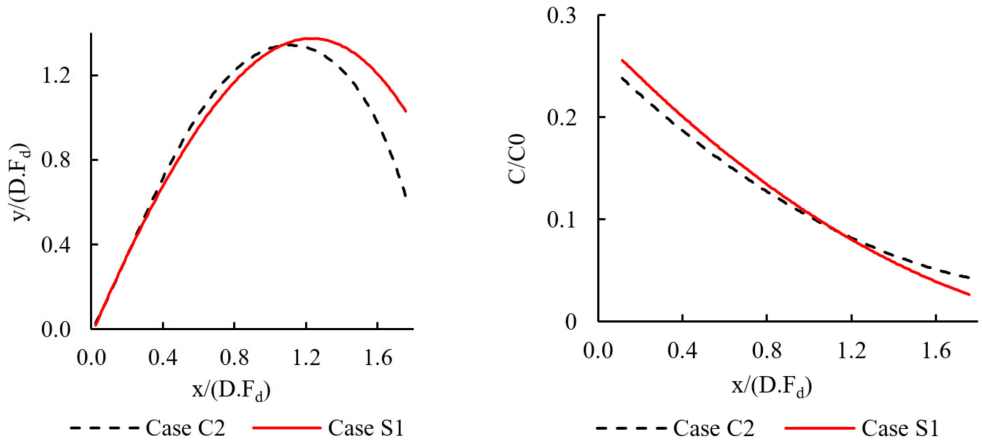

Figure 11. (**a**) Trajectory and (**b**) concentration of the central jet of cases C2 and S1.

To evaluate the overall effect of non-uniform port orientation, the concentration downstream of the impact point of all jets were investigated. Particularly, the concentration at $x/(D.F_d) = 3.4$ and the elevation of nozzle tip on the centerline planes of central and adjacent jets are shown in Figure 12. According to Figure 12, the concentration beyond the impact point on the central jet of case S1 was 3.7% lower than that on the central jet of case C2. Additionally, the concentration on the planes of adjacent jets for the non-uniform case was 8.4% lower compared to that for the uniform case. Therefore, the results show some improvements in dilution when adopting the multiport diffuser with non-uniform port orientation compared to the uniform diffuser.

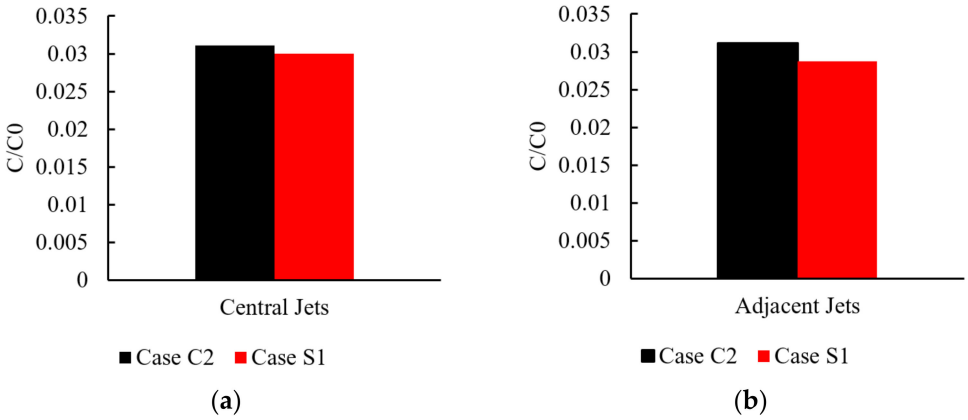

Figure 12. Concentration at $x/(D.F_d) = 3.4$ and the elevation of nozzle tip on the centerline planes of (**a**) central and (**b**) adjacent jets.

4. Conclusions

The first aim of the present study was to evaluate the prediction capabilities of RSMs for multiple inclined dense jets. The LRR turbulence model, as a new approach for multiple jets, was employed to perform the simulations. The predictions of geometrical characteristics and impact dilution were compared to the existing experimental measurements. Subsequently, the validated model was applied to perform further investigations on the effect of non-uniform port orientation on the merging process of multiple inclined dense jets, as a novel contribution. Particularly, diffusers with uniform, 60°–60°–60°, and non-uniform, 45°–60°–45°, port orientation were considered, and the effect of adjacent ports on the central ports was determined.

It was found that the LRR turbulence model, as an RSM, can be a reliable model for the study of the mixing behavior of multiple inclined dense jets, and can provide results of geometrical characteristics and impact dilution within the range of 5% and 7%, respectively. It also provides more accurate results compared to the EVMs including the standard and RNG k-ε turbulence models. Furthermore, the comparison of the diffuser with uniform and non-uniform port orientation showed that jet merging process is significantly affected by the port's orientation and the middle discharge may have a longer trajectory and therefore a higher dilution rate when its adjacent jets are discharged at a different angle, compared to that of uniform discharges. The terminal rise height, impact distance, and impact dilution of the central jet on a diffuser with uniform port inclination were found to be 7%, 5%, and 14% higher than those of the uniform case, respectively. It can be concluded that the behavior of the central jet on the diffuser with non-uniform port orientation is more like a single jet, compare to the one with uniform ports. Generally, the effects of jet merging and dynamic interactions on the central jet, including inward bending and a reduction in geometrical characteristics, are more significant when the nozzles are uniform. The evaluation of the overall effects of non-uniform port orientation showed 3.7% to 8.4% increment in dilution beyond the impact point.

This study showed how the trajectory and dilution of the middle discharge were affected by the orientation of its adjacent jets and how merging process was influenced by the orientation. The results of this study can be of interest in practical projects applying multiport diffusers to discharge brine or saline water as a by-product of osmotic power plants and municipal dense wastewaters into water bodies. A change in port orientation may provide an inexpensive way to augment dilution, compared to costly methods such as an increase in port spacing. This study highlighted the effects of non-uniform port orientation on merging process of multiple dense jets in near-field; however, the effect of non-uniform port orientation on intermediate and far fields may also be of interest. The outcomes have the potential to be considered by outfall designers. More investigations on the other parameters, such as flowing current, stratification, along with port orientation, are also recommended.

Author Contributions: Conceptualization, A.M. and S.A.R.S.H.; methodology, A.M.; software, S.A.R.S.H. and A.M.; validation, S.A.R.S.H.; formal analysis, S.A.R.S.H.; investigation, S.A.R.S.H.; resources, S.A.R.S.H.; data curation, S.A.R.S.H., A.M., P.J.W.R. and O.A.; writing—original draft preparation, S.A.R.S.H.; writing—review and editing, A.M., P.J.W.R. and O.A.; visualization, S.A.R.S.H.; supervision, A.M.; project administration, A.M.; funding acquisition, A.M. All authors have read and agreed to the published version of the manuscript.

Funding: This research was funded by Natural Sciences and Engineering Research Council of Canada (NSERC), grant number 210717. The research of S.A.R.S.H. was supported by Mitacs through the Mitacs Research Training Award.

Institutional Review Board Statement: Not applicable.

Informed Consent Statement: Not applicable.

Data Availability Statement: Not applicable.

Conflicts of Interest: The authors declare no conflict of interest.

References

1. Einav, R.; Lokiec, F. Environmental aspects of a desalination plant in Ashkelon. *Desalination* **2003**, *156*, 79–85. [CrossRef]
2. Lai, C.; Zhao, B.; Law, A.W.K.; Adams, E.E. A numerical and analytical study of the effect of aspect ratio on the behavior of a round thermal. *Environ. Fluid Mech.* **2015**, *15*, 85–108. [CrossRef]
3. Yan, X.; Mohammadian, A. Numerical Modeling of Multiple Inclined Dense Jets Discharged from Moderately Spaced Ports. *Water* **2019**, *11*, 2077. [CrossRef]
4. Lyu, S.; Seo, I.W.; Kim, Y.D. Experimental investigation on behavior of multiple vertical buoyant jets discharged into a stagnant ambient. *KSCE J. Civ. Eng.* **2013**, *17*, 1820–1829. [CrossRef]
5. Wang, H.J.; Davidson, M.J. Jet Interaction in a Still Ambient Fluid. *J. Hydraul. Eng.* **2003**, *129*, 349–357. [CrossRef]
6. Knystautas, R. The Turbulent Jet from a Series of Holes in Line. *Aeronaut. Q.* **1964**, *15*, 1–28. [CrossRef]

7. Liseth, P. Mixing of merging buoyant jets from a manifold in stagnant receiving water of uniform density. In *Advances in Water Pollution Research, Proceedings of the Sixth International Conference, Munich, Germany, 1 January 1973*; Pergamon Press: Oxford, UK, 1973; pp. 921–936.
8. Seo, I.W.; Yeo, H.K. Near-field dilution of rosette type multiport wastewater diffusers. *Water Eng. Res. Int. J. Kings Waste Recycl. Auth.* **2002**, *3*, 93–111.
9. Tian, X.; Roberts, P.J.W.; Daviero, G.J. Marine wastewater discharges from multiport diffusers. I: Unstratified stationary water. *J. Hydraul. Eng.* **2004**, *130*, 1137–1146. [CrossRef]
10. Tian, X.; Roberts, P.J.W. Experiments on Marine Wastewater Diffusers with Multiport Rosettes. *J. Hydraul. Eng.* **2011**, *137*, 1148–1159. [CrossRef]
11. Roberts, P.J.W.; Hunt, C.D.; Mickelson, M.J.; Tian, X. Field and Model Studies of the Boston Outfall. *J. Hydraul. Eng.* **2011**, *137*, 1415–1425. [CrossRef]
12. Yannopoulos, P.C.; Noutsopoulos, G.C. Interaction of vertical round turbulent buoyant jets—Part I: Entrainment restriction approach. *J. Hydraul. Res.* **2006**, *44*, 218–232. [CrossRef]
13. Koh, R.C.Y.; Fan, L.N. Mathematical models for the prediction of temperature distributions resulting from the discharge of heated water in large bodies of water. *EPA Water Pollut. Control. Res. Ser.* **1970**, 16130. Available online: https://aquadocs.org/bitstream/handle/1834/25305/EPA_Koh.PDF?sequence=1&isAllowed=y (accessed on 20 April 2022).
14. Hodgson, J.E.; Moawad, A.K.; Rajaratnam, N. Concentration field of multiple circular turbulent jets. *J. Hydraul. Res.* **1999**, *37*, 249–256. [CrossRef]
15. Yannopoulos, P.C.; Noutsopoulos, G.C. Interaction of vertical round turbulent buoyant jets—Part II: Superposition method. *J. Hydraul. Res.* **2006**, *44*, 233–248. [CrossRef]
16. Lai, A.C.H.; Lee, J.H.W. Dynamic interaction of multiple buoyant jets. *J. Fluid Mech.* **2012**, *708*, 539–575. [CrossRef]
17. Adams, E.E. Submerged Multiport Diffusers in Shallow Water with Current. Ph.D. Thesis, Massachusetts Institute of Technology, Cambridge, MA, USA, 1972.
18. Marti, C.L.; Antenucci, J.P.; Luketina, D.; Okely, P.; Imberger, J. Near-Field Dilution Characteristics of a Negatively Buoyant Hypersaline Jet Generated by a Desalination Plant. *J. Hydraul. Eng.* **2011**, *137*, 57–65. [CrossRef]
19. Abessi, O.; Roberts, P.J.W. Multiport Diffusers for Dense Discharges. *J. Hydraul. Eng.* **2014**, *140*, 04014032. [CrossRef]
20. Abessi, O.; Roberts, P.J.W. Multiport Diffusers for Dense Discharge in Flowing Ambient Water. *J. Hydraul. Eng.* **2017**, *143*, 04017003. [CrossRef]
21. Abessi, O.; Roberts, P.J.W. Rosette Diffusers for Dense Effluents in Flowing Currents. *J. Hydraul. Eng.* **2018**, *144*, 06017024. [CrossRef]
22. Shrivastava, I.; Adams, E.E. Mixing of Tee Diffusers in Shallow Water with Crossflow: A New Look. *J. Hydraul. Eng.* **2019**, *145*, 04019006. [CrossRef]
23. Xu, Z.; Otoo, E.; Chen, Y.; Ding, H. 2D PIV Measurement of Twin Buoyant Jets in Wavy Cross-Flow Environment. *Water* **2019**, *11*, 399. [CrossRef]
24. Lee, J.H.W.; Cheung, V. Generalized Lagrangian Model for Buoyant Jets in Current. *J. Environ. Eng.* **1990**, *116*, 1085–1106. [CrossRef]
25. Lee, J.H.W.; Chu, V.H. *Turbulent Jets and Plumes: A Lagrangian Approach*; Springer Science & Business Media: Berlin/Heidelberg, Germany, 2003; Volume 1.
26. Jirka, G.H. Integral Model for Turbulent Buoyant Jets in Unbounded Stratified Flows. Part I: Single Round Jet. *Environ. Fluid Mech.* **2004**, *4*, 1–56. [CrossRef]
27. Frick, W.E. Visual Plumes mixing zone modeling software. *Environ. Model. Softw.* **2004**, *19*, 645–654. [CrossRef]
28. Taherian, M.; Mohammadian, A. Buoyant Jets in Cross-Flows: Review, Developments, and Applications. *J. Mar. Sci. Eng.* **2021**, *9*, 61. [CrossRef]
29. Baum, M.J.; Gibbes, B. Field-Scale Numerical Modeling of a Dense Multiport Diffuser Outfall in Crossflow. *J. Hydraul. Eng.* **2020**, *146*, 05019006. [CrossRef]
30. Roberts, P.J.W. Near Field Flow Dynamics of Concentrate Discharges and Diffuser Design. *Subser. Environ. Sci.* **2015**, *149*, 369–396. [CrossRef]
31. Palomar, P.; Lara, J.; Losada, I. Near field brine discharge modeling part 2: Validation of commercial tools. *Desalination* **2012**, *290*, 28–42. [CrossRef]
32. Taherian, M.; Saeidi Hossein, S.A.R.; Mohammadian, A. Overview of outfall discharge modeling with a focus on turbulence modeling approaches. In *Advances in Fluid Mechanics: Modeling and Simulation*; Springer: Singapore, 2022; ISSN 2364-6748.
33. Ardalan, H.; Vafaei, F. CFD and Experimental Study of 45° Inclined Thermal-Saline Reversible Buoyant Jets in Stationary Ambient. *Environ. Process.* **2019**, *6*, 219–239. [CrossRef]
34. Gildeh, H.K.; Mohammadian, A.; Nistor, I.; Qiblawey, H. Numerical Modeling of Turbulent Buoyant Wall Jets in Stationary Ambient Water. *J. Hydraul. Eng.* **2014**, *140*, 04014012. [CrossRef]
35. Gildeh, H.K.; Mohammadian, A.; Nistor, I.; Qiblawey, H. Numerical modeling of 30° and 45° inclined dense turbulent jets in stationary ambient. *Environ. Fluid Mech.* **2014**, *15*, 537–562. [CrossRef]
36. Gildeh, H.K.; Mohammadian, A.; Nistor, I.; Qiblawey, H.; Yan, X. CFD modeling and analysis of the behavior of 30° and 45° inclined dense jets—New numerical insight. *J. Appl. Water Eng. Res.* **2016**, *4*, 112–127. [CrossRef]

37. Huai, W.-X.; Li, Z.-W.; Qian, Z.; Zeng, Y.-H.; Han, J.; Peng, W.-Q. Numerical Simulation of Horizontal Buoyant Wall Jet. *J. Hydrodyn.* **2010**, *22*, 58–65. [CrossRef]
38. Oliver, C.J.; Davidson, M.J.; Nokes, R.I. k-ε Predictions of the initial mixing of desalination discharges. *Environ. Fluid Mech.* **2008**, *8*, 617–625. [CrossRef]
39. Zhang, S.; Jiang, B.; Law, A.W.-K.; Zhao, B. Large eddy simulations of 45° inclined dense jets. *Environ. Fluid Mech.* **2015**, *16*, 101–121. [CrossRef]
40. Zhang, S.; Law, W.K.A.; Jiang, M. Large eddy simulations of 45° and 60° inclined dense jets with bottom impact. *J. Hydro-environ. Res.* **2017**, *15*, 54–66. [CrossRef]
41. Jiang, M.; Law, A.W.-K.; Lai, A.C.H. Turbulence characteristics of 45° inclined dense jets. *Environ. Fluid Mech.* **2018**, *19*, 27–54. [CrossRef]
42. Xue, W.; Huai, W.-X.; Qian, Z.; Yang, Z.; Zeng, Y. Numerical simulation of initial mixing of marine wastewater discharge from multiport diffusers. *Eng. Comput.* **2014**, *31*, 1379–1400. [CrossRef]
43. Tang, H.S.; Paik, J.; Sotiropoulos, F.; Khangaonkar, T. Three-Dimensional Numerical Modeling of Initial Mixing of Thermal Discharges at Real-Life Configurations. *J. Hydraul. Eng.* **2008**, *134*, 1210–1224. [CrossRef]
44. Yan, X.; Ghodoosipour, B.; Mohammadian, A. Three-Dimensional Numerical Study of Multiple Vertical Buoyant Jets in Stationary Ambient Water. *J. Hydraul. Eng.* **2020**, *146*, 04020049. [CrossRef]
45. Fischer, H.B.; List, E.J.; Koh, R.C.Y.; Imberger, J.; Brooks, N.H. *Mixing in Inland and Coastal Waters*; Academic Press: Amsterdam, The Netherlands, 1979.
46. Roberts, P.J.W.; Ferrier, A.; Daviero, G. Mixing in Inclined Dense Jets. *J. Hydraul. Eng.* **1997**, *123*, 693–699. [CrossRef]
47. Missimer, T.M.; Jones, B.; Maliva, R.G. *Intakes and Outfalls for Seawater Reverse-Osmosis Desalination Facilities: Innovations and Environmental Impacts*; Springer: New York, NY, USA, 2015.
48. Kikkert, G.A.; Davidson, M.J.; Nokes, R.I. Inclined Negatively Buoyant Discharges. *J. Hydraul. Eng.* **2007**, *133*, 545–554. [CrossRef]
49. Zeitoun, M.; McIlhenny, W. Conceptual Designs of Outfall Systems for Desalination Plants. In *Offshore Technology Conference*; OnePetro: Washington, DC, USA, 1970.
50. Zeitoun, M.A.; McHilhenny, W.F. *Model Studies of Outfall Systems for Desalination Plants; Part III. Numerical Simulation and Design Considerations*; Dow Chemical Co.: Freeport, TX, USA, 1972; Available online: https://www.tib.eu/de/suchen/id/ntis:sid~{}oai:ds2:ntis/5319e8d74fe2d5c13d04dc1c/Model-Studies-of-Outfall-Systems-for-Desalination?tx_tibsearch_search%5Bsearchspace%5D=tn&cHash=7fcf481ee07b3258c85f7bc313ad0c16 (accessed on 20 April 2022).
51. Abessi, O.; Roberts, P.J.W. Effect of Nozzle Orientation on Dense Jets in Stagnant Environments. *J. Hydraul. Eng.* **2015**, *141*, 06015009. [CrossRef]
52. Lim, A.; Lam, Y. Numerical Investigation of Nanostructure Orientation on Electroosmotic Flow. *Micromachines* **2020**, *11*, 971. [CrossRef] [PubMed]
53. Lim, A.E.; Lam, Y.C. Vertical Squeezing Route Taylor Flow with Angled Microchannel Junctions. *Ind. Eng. Chem. Res.* **2021**, *60*, 14307–14317. [CrossRef]
54. Roberts, P.J.W.; Toms, G. Inclined Dense Jets in Flowing Current. *J. Hydraul. Eng.* **1987**, *113*, 323–340. [CrossRef]
55. Versteeg, H.K.; Malalasekera, W. *An Introduction to Computational Fluid Dynamics: The Finite Volume Method, 2nd ed*; Pearson Education: London, UK, 2007.
56. Peyret, R.; Krause, E. (Eds.) *Advanced Turbulent Flow Computations*; Springer: Wien, Austria, 2000.
57. Hanjalic, K. *Closure Models for Incompressible Turbulent Flows*; Lecture Notes at Von Kármán Institute: Brussels, Belgium, 2004; p. 75.
58. Abessi, O.; Saeedi, M.; Davidson, M.; Zaker, N.H. Flow Classification of Negatively Buoyant Surface Discharge in an Ambient Current. *J. Coast. Res.* **2012**, *278*, 148–155. [CrossRef]
59. Lai, C.C.; Lee, J.H. Mixing of inclined dense jets in stationary ambient. *J. Hydro Environ. Res.* **2012**, *6*, 9–28. [CrossRef]
60. Roberts, P.J.W.; Toms, G. Ocean outfall system for dense and buoyant effluents. *J. Environ. Eng.* **1988**, *114*, 1175–1191.
61. Holzmann, T. *Mathematics, Numerics, Derivations and OpenFOAM®*; Holzmann CFD: Loeben, Germany, 2016.
62. Killingstad, P.E. A Study of Dead Water Resistance Reynolds Averaged Navier Stokes Simulations of a Barge Moving in Stratified Waters. Master's Thesis, University of Oslo, Oslo, Norway, 2018. Available online: https://www.duo.uio.no/bitstream/handle/10852/63458/Peter_Killingstad_masterThesis.pdf?sequence=1&isAllowed=y (accessed on 20 April 2022).
63. Launder, B.E.; Reece, G.J.; Rodi, W. Progress in the development of a Reynolds-stress turbulence closure. *J. Fluid Mech.* **1975**, *68*, 537–566. [CrossRef]
64. Lauria, A.; Alfonsi, G.; Tafarojnoruz, A. Flow Pressure Behavior Downstream of Ski Jumps. *Fluids* **2020**, *5*, 168. [CrossRef]
65. Tafarojnoruz, A.; Lauria, A. Large eddy simulation of the turbulent flow field around a submerged pile within a scour hole under current condition. *Coast. Eng. J.* **2020**, *62*, 489–503. [CrossRef]
66. Calomino, F.; Alfonsi, G.; Gaudio, R.; D'Ippolito, A.; Lauria, A.; Tafarojnoruz, A.; Artese, S. Experimental and numerical study of free-surface flows in a corrugated pipe. *Water* **2018**, *10*, 638. [CrossRef]
67. Palomar, P.; Lara, J.; Losada, I.; Rodrigo, M.; Alvárez, A. Near field brine discharge modelling part 1: Analysis of commercial tools. *Desalination* **2012**, *290*, 14–27. [CrossRef]
68. Yan, X.; Mohammadian, A. Numerical Modeling of Vertical Buoyant Jets Subjected to Lateral Confinement. *J. Hydraul. Eng.* **2017**, *143*, 04017016. [CrossRef]

69. Yan, X.; Mohammadian, A.; Chen, X. Three-Dimensional Numerical Simulations of Buoyant Jets Discharged from a Rosette-Type Multiport Diffuser. *J. Mar. Sci. Eng.* **2019**, *7*, 409. [CrossRef]
70. OpenFOAM. *The OpenFOAM Foundation*; OpenCFD Ltd.: Bracknell, UK, 2015.
71. Li, Y.; Geng, X.; Wang, H.; Zhuang, X.; Ouyang, J. Simulating the frontal instability of lock-exchange density currents with dissipative particle dynamics. *Mod. Phys. Lett. B* **2016**, *30*, 1650200. [CrossRef]
72. Shao, D.; Adrian, W.K.L. Mixing and boundary interactions of 30 and 45 inclined dense jets. *Environ. Fluid Mech.* **2010**, *10*, 521–553. [CrossRef]
73. Roberts, P.J.W.; Snyder, W.H.; Baumgartner, D.J. Ocean Outfalls. III: Effect of Diffuser Design on Submerged Wastefield. *J. Hydraul. Eng.* **1989**, *115*, 49–70. [CrossRef]